



Removal of chloramphenicol from aqueous solution by nanoscale zero-valent iron particles



Siqing Xia^a, Zaoli Gu^{a,b}, Zhiqiang Zhang^{a,b,*}, Jiao Zhang^c, Slawomir W. Hermanowicz^{d,e}

^a State Key Laboratory of Pollution Control and Resource Reuse, College of Environmental Science and Engineering, Tongji University, Shanghai 200092, China

^b Key Laboratory of Yangtze River Water Environment, Ministry of Education, College of Environmental Science and Engineering, Tongji University, Shanghai 200092, China

^c School of Civil Engineering and Transportation, Shanghai Technical College of Urban Management, Shanghai 200432, China

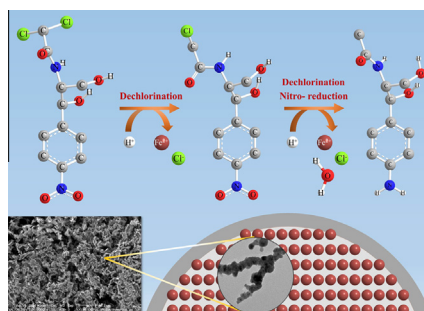
^d Department of Civil and Environmental Engineering, University of California, Berkeley, 629 Davis Hall #1710, Berkeley, CA 94720-1710, USA

^e National High-end Foreign Expert Program, Tongji University, Shanghai 200092, China

HIGHLIGHTS

- Chloramphenicol (CAP) removal by nanoscale zero-valent iron (nZVI) was investigated.
- Effects of dosage, initial pH and air on chloramphenicol removal were ascertained.
- Removal kinetics model of CAP by nZVI was constructed.
- Removal mechanisms of CAP by nZVI were disclosed via various analyzing techniques.
- Rational reduction pathway of CAP by nZVI was provided.

GRAPHICAL ABSTRACT



ARTICLE INFO

Article history:

Received 22 April 2014

Received in revised form 21 June 2014

Accepted 25 June 2014

Available online 9 July 2014

Keywords:

Chloramphenicol
Nanoscale zero-valent iron
Removal kinetics
Reduction pathway

ABSTRACT

The chloramphenicol (CAP) removal from aqueous solution by nanoscale zero-valent iron (nZVI) particles was systematically investigated using batch experiments. The effects of the key parameters including nZVI dosage, initial pH and air on the CAP removal were ascertained. The removal process of CAP followed a pseudo-first order kinetics model. The removal efficiency was found to be enhanced with increasing nZVI dosage and decreasing initial pH. Due to the Fenton reaction of the nZVI catalyzed by the oxygen in the air, the nZVI process with air showed higher CAP removal efficiency than that with N₂. Under the conditions of nZVI dosage 1.06 g/L, initial pH 6.8 and air presence, CAP (100 mg/L) was completely removed by nZVI within 5 min. The Raman analyses of nZVI particles before and after the process indicated that CAP was adsorbed and reduced on the surface of nZVI particles. The XPS analyses along with the ICP results further confirmed that Fe⁰ was oxidized after the process. From the LC-MS and GC-MS results of the CAP reduction products, dechlorination followed by nitro group reduction was proposed to be the potential reduction routine of CAP by nZVI.

© 2014 Elsevier B.V. All rights reserved.

1. Introduction

Contamination by pharmaceuticals and personal care products (PPCPs) in surface water and ground water are emerging as a

potential threat to the ecosystem and human health [1,2]. PPCPs, especially pharmaceuticals, are reported to act as an inhibitor of multi-xenobiotic resistance, which creates adverse effects on aquatic organisms [3]. Due to antibiotic effects and their high molecular

* Corresponding author at: State Key Laboratory of Pollution Control and Resource Reuse, College of Environmental Science and Engineering, Tongji University, Shanghai 200092, China. Tel.: +86 21 65981831.

E-mail address: zhiqiang@tongji.edu.cn (Z. Zhang).

complexity, these contaminants usually cannot be removed effectively by conventional wastewater treatment methods [3,4]. Accordingly, a great deal of efforts are being made to find out ways of inactivating or eliminating this class of substances in surface water or wastewater [5–7].

Among the medicines, antibiotics receives extensive concern because of a wide usage all over the world [8]. Chloramphenicol (CAP, Fig. 1) is a broad-spectrum antibiotic with excellent antibacterial properties, isolated from *Streptomyces venezuelae* in 1947. Inhibiting protein synthesis in microorganisms, CAP is effective against Gram-positive and Gram-negative cocci and bacilli, which makes it a popular choice to treat human and animal diseases [9]. Various side effects of CAP, however, were revealed, e.g., fatal bone marrow depression and aplastic anemia [10]. It is reported that the detected concentrations of CAP in municipal sewage, the Nanming River and the sediment of Nanming River of Guiyang City, China were up to 47.4 µg/L, 19.0 µg/L and 1138 µg/kg, respectively [11]. In Germany, CAP was also found in sewage treatment plant effluents and river water at concentrations up to 0.56 and 0.06 µg/L, respectively [12]. Up to present, only a few studies on CAP removal from water or wastewater have been reported. Chatzidakis et al. [13] and Zhang et al. [14] reported photo-catalytic oxidation of CAP by TiO₂, while radiation induced CAP removal was also reported by Kapoor and Varshney [15] and Csay et al. [16]. However, the products of CAP during photocatalytic degradation and irradiation might be more toxic for human health [17]. Moreover, great investments in infrastructure limit their applications for large scale operations [18]. Fan et al. [19] reported using bamboo charcoal as an adsorbent to remove CAP from wastewater. During this process, CAP is simply accumulated and then separated from water without any degradation, which was unsatisfactory in the field of pollution abatement [18]. Development of new techniques like nanotechnology may help solving this problem.

Nanotechnology is one of the most rapidly growing sectors of the global economy. For the treatment of persistent pollutants, a growing body of theoretical and empirical evidences have proven that nanoscale zero-valent iron (nZVI) particles are both highly effective and versatile due to their high specific surface area, environmental harmlessness and capabilities for catalytic reduction of contaminants [20]. The removing mechanism of contaminant by nZVI is still unclear and several mechanisms have been proposed: reduction, oxidation, adsorption and co-precipitation. In terms of reduction, the dehalogenation mechanism of nZVI in aqueous solution is a multi-step process depending on the target substances. Fe⁰ acts as an electron donor to reduce organic pollutants [21]. As for the oxidation process, in the Fe⁰–H₂O system, strong oxidants are generated in the presence of oxygen, including hydroxyl radicals, ferryl ions, and superoxide radicals. In the oxidation process with nZVI under aerobic conditions, hydrogen peroxide (H₂O₂) is produced as an intermediate product and the desorbed H₂O₂ is able to react with ferrous iron following the Fenton reactions (Eqs. 1–3) [22–24]. For adsorption and co-precipitation, iron hydroxides or oxides are formed on the surface of nZVI, which are well known for their adsorption capacities [25]. To the best of our knowledge, the CAP removal from aqueous solution by nZVI has not been

reported previously. Therefore, it appears interesting to investigate the efficacy of this novel technique and its mechanisms.



The present study is aimed to investigate the removal mechanisms of CAP from aqueous solution by nZVI. The effects of the key parameters including nZVI dosage, initial pH, and air on the CAP removal were examined to study removal kinetics. Several techniques, including XPS, Raman, ICP, LC–MS and GC–MS, were used to obtain the structural features of CAP reduction products and further analyze the removal mechanisms.

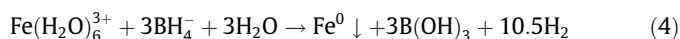
2. Materials and methods

2.1. Materials

Sodium borohydride (NaBH₄, Analytical Reagent), ferric chloride hexahydrate (FeCl₃·6H₂O, Analytical Reagent) and ethanol (C₂H₅OH, Analytical Reagent) were purchased from Sinopharm Chemical Reagent Shanghai Co., Ltd. (China); chloramphenicol (C₁₁H₁₂Cl₂N₂O₅, Analytical Reagent) was obtained from Sangon Biotech Shanghai Co., Ltd. (China); acetonitrile (CH₃CN, HPLC grade), methanol (CH₃OH, HPLC grade), N-Hexane (C₆H₁₄, HPLC grade) and formic acid (HCOOH, HPLC grade) was from Shanghai ANPEL Scientific Instrument Co., Ltd. (China). Chloramphenicol standard used for establishing standard curve was obtained from Dr. Ehrenstorfer GmbH (Germany). Bis(trimethylsilyl)trifluoroacetamide trimethylchlorosilane (BSTFA:TMCS, 99:1) was purchased from Regis Technologies, Inc. (USA).

2.2. nZVI preparation

The nZVI particles were prepared via a liquid phase reduction method described by Wang and Zhang [26]. Deionized water was deoxygenated by purging with N₂ for 30 min before use. nZVI particles were produced by adding 1.6 M NaBH₄ aqueous solution dropwise to a 1.0 M FeCl₃·6H₂O aqueous solution at ambient temperature with vigorous stirring. Ferric iron (Fe³⁺) was reduced according to the following reaction [27]:



The synthesized nZVI particles were washed with deoxygenated deionized water and pure ethanol three times and stored in ethanol for further use.

2.3. Characterization analyses of nZVI

Prior to the measurements, nZVI particles were dried using a vacuum freeze-drying method. The measurement of specific surface area of nZVI was performed using a nitrogen adsorption isotherm with a specific surface area pore size analyzer (JW BK122W, Beijing JWGB Sci & Tech Co., Ltd., China). The surface, morphology and size of nZVI were examined using scanning electron microscopy (SEM, XL-10, Koninklijke Philips N.V., Netherland) and transmission electron microscopy (TEM, JEM-2011, Jeol, Japan). The crystal structures of prepared nanoparticles were examined with X-ray powder diffraction (XRD, D8 Advance X, BRUKER AXS GMBH, Germany). Elemental composition of nZVI was determined with XPS (PHI 5000C ESCA, Physical Electronics, Inc., USA).

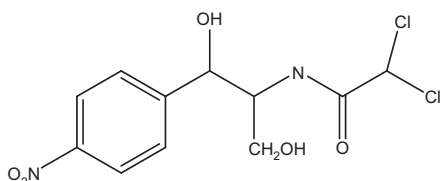


Fig. 1. Chemical structure of CAP.

2.4. CAP removal by nZVI

Batch experiments of CAP removal were performed in 50-mL serum bottles. The benchmark experiment conditions were as follows: nZVI dosage 1.06 g/L, initial pH 6.8, and air presence. For better comparison with the former researches regarding the removal of CAP with other techniques [19,28] and the removal of other antibiotics by nZVI [29,30], a similar concentration of CAP (100 mg/L) was applied. Previously prepared nZVI particles were introduced into the bottles, and CAP aqueous solution (40 mL) was added and mixed on a rotary shaker at ambient temperature (25 ± 1 °C). Periodically, 0.25 mL of the aqueous solution was withdrawn with a 1-mL gas-tight syringe into a 2-mL vial and filtered immediately through a 0.45 μm membrane filter for HPLC analysis.

2.5. Analytical methods of products

The concentration of CAP in the solution was analyzed using high performance liquid chromatography (LC-20AT, Shimadzu Corporation, Japan) equipped with a photo-diode array detector (SPD-M20A) and a C18 column (250 mm \times 4.6 mm \times 5 μm , VP-ODS) at the following conditions: mobile phase: 35% acetonitrile and 65% water, flow rate: 1.0 mL/min, injection volume: 20 μL , column temperature: 40 °C, absorbance detection: 277 nm. The retention times for CAP is 7.24 min and the correlation coefficient of the standard curve ($n = 6$) was greater than 0.9999.

The concentration of soluble Fe was tested with an inductive coupled plasma emission spectrometer (ICP-720ES, Agilent Technologies, Inc., USA) with RF power = 1.35 kW.

Dissolved oxygen (DO) and pH were detected by a multi-parameter potable meter (HQ40d, Hach, USA) equipped with a luminescent/optical dissolved oxygen probe (IntelliCAL LDO101, Hach) and a gel filled pH electrode (IntelliCAL PHC101, Hach).

HPLC-ESI-MS measurements were carried out using a liquid chromatography-triple stage quadrupole mass spectrometer (TSQ Quantum Access MAX, Thermo Fisher Scientific Inc., USA) equipped with a C18 column (150 mm \times 2.1 mm \times 3.5 μm , Eclipse Plus, Agilent Technologies, Inc., USA). Mobile phase: 0.1% formic acid-water (A) and 0.1% formic acid-acetonitrile (B). The gradient profile was carried out starting from 5% to 50% of B in 30 min, then to 90% of B in 0.5 min, held for 5 min, and then to 10% of B in 0.5 min, held for 5 min, at a flow rate of 0.2 mL/min and an injection volume of 5 μL . MS data acquisition was performed in the Full Scan/Q1MS mode. In order to obtain maximum sensitivity for identification and detection of CAP, the ion spray voltage was always set at 4.0 kV.

GC-EI-MS measurements were carried out using a gas chromatography-triple stage quadrupole mass spectrometer (TSQ Quantum XLS, Thermo Fisher Scientific Inc., USA) equipped with a

5%-phenyl-film column (30 m \times 0.25 mm \times 0.25 μm , TraceGOLD TG-5MS). The samples were extracted with Ploy-Sery HLB SPE tube (CNW, China), derivatized using BSTFA:TMCS (99:1) and then dissolved in N-Hexane before injection. For the GC the following conditions were used: Initial 80 °C, held for 2 min, ramp 8.0 °C/min to 300 °C, held for 2.0 min, at a He flow rate of 1.0 mL/min. MS data acquisition was performed in the Full Scan/Q1MS mode with source temperature 240 °C, emission current 50 μA , transfer Line 310 °C and injection volume 1 μL .

3. Results and discussion

3.1. nZVI characterization

The morphology and size of the synthesized nZVI particles are shown in the SEM and TEM images (Fig. 2). The nZVI particles had a core-shell structure with particle size in a range of 20–50 nm. The particles formed a chainlike, aggregated structure because of magnetic interactions between them and a natural tendency to remain in more thermodynamically stable state [31]. The synthesized nZVI had a BET surface area of 32.02 m^2/g and a BJH adsorption average pore diameter of 8.04 nm, which was similar to the values of other researches [32]. Compared to commercial iron powder, the synthesized nZVI was much smaller in diameter and higher in BET surface area. Those differences enhanced the nZVI activity and made it attractive for eliminating contaminants. According to the XRD pattern of the synthesized nZVI particles shown in Fig. 2c, there was a broad peak at the 2θ incidence angle of 44.662°. It indicated the presence of Fe^0 that possessed an amorphous structure.

3.2. Removal kinetics of CAP by nZVI

Kinetic experiments with varying parameters (amount of nZVI added and solution pH) were used to estimate an observed reaction rate coefficient k_{obs} (Eq. 5), where c is the CAP concentration (mg/L), t the time (s) and k_{obs} the observed reaction rate coefficient (s^{-1}). As shown in Fig. 3, the overall removal process did not exactly follow the pseudo-first-order kinetics. In the beginning, the removal rate of CAP was faster than that in the later, possibly due to an initial sorption process [33]. This indicated that the removal mechanisms were more complicated than that suggested by Eq. 5. However, as a tool to analyze the results, rate coefficients obtained by this way were still significant and comparable.

$$\frac{dc}{dt} = -k_{\text{obs}}c \quad (5)$$

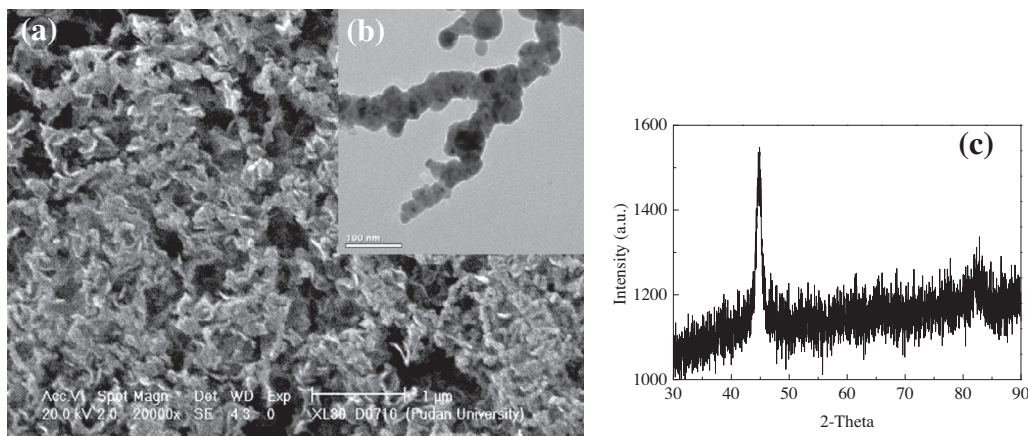


Fig. 2. (a) SEM image of the synthesized nZVI, (b) TEM image of the synthesized nZVI and (c) characterization of nZVI particles by XRD.

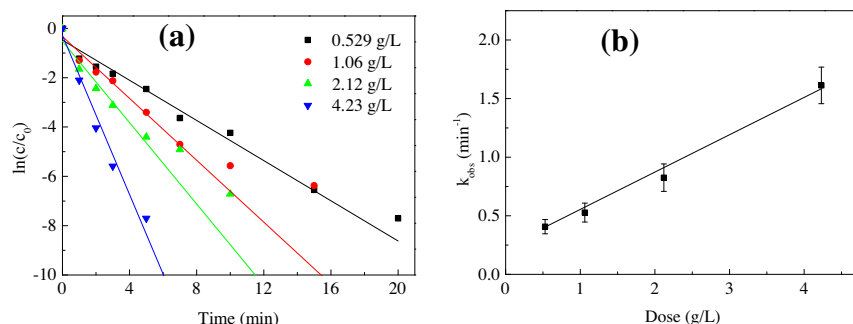


Fig. 3. (a) Effects of variations in nZVI dosage on the removal of CAP (experimental conditions: initial pH = 6.8, initial CAP conc. = 110 mg/L, shaking speed = 150 rpm, 25 ± 1 °C); (b) relationship between nZVI dosage and observed rate coefficients.

3.2.1. Effect of nZVI dosage on CAP removal

The effect of nZVI dosage (0.53, 1.06, 2.12 and 4.23 g/L) on the CAP (initial concentration 100 mg/L) removed by nZVI was studied (Fig. 3a). The plot of k_{obs} and nZVI dosage presented their linear dependence (Fig. 3b). The removal efficiency of CAP was greatly enhanced with the increase of nZVI dosage. This enhancement was due to the catalytic reduction occurring on the surface of nZVI and increasing available surface area for adsorption and reaction sites [26]. The nZVI presented extremely great capability of catalytic reduction because of its small diameter and huge surface area, which have been earlier demonstrated with TEM and BET.

3.2.2. Effect of initial pH on CAP removal

The solution pH is considered as one of the most important factors affecting the removal process of organic contaminants with nZVI. The CAP removal was examined for a series of initial pH values (2.8, 4.8, 6.8, 8.8 and 10.8). Fig. 4a shows that the removal followed the pseudo-first-order kinetics at a given pH value, and as shown in Fig. 4b, increasing initial solution pH value led to a remarkable decrease in k_{obs} . Thus, acidic conditions were favorable for CAP removal by nZVI. The result was similar to the previous reports [18,34]. This effect was ascribed to the fact that: (a) at lower pH values, the iron corrosion could be accelerated, producing abundant hydrogen for hydrogenation reactions [35]; (b) at higher solution pH, a passive film of iron hydroxide formed on the surfaces of nanoparticles, which could inhibit further reactions [36].

3.2.3. Comparison of nZVI/air process and nZVI/N₂ process

The CAP removal by nZVI were conducted under air conditions and nitrogen conditions (bubbling N₂ for 10 min before reaction), respectively, at pH 6.8, initial CAP concentration of 110 mg/L, and nZVI dosage of 1.0 g/L. The results shown in Fig. 5 indicated that the removal efficiency under air presence was much higher than that under nitrogen presence, which indicate that oxygen served

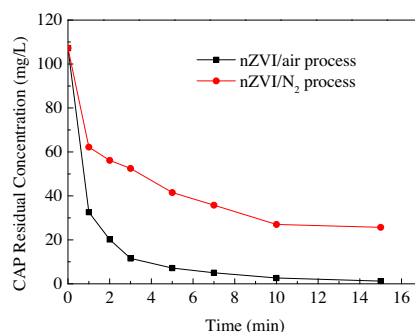


Fig. 5. Effects of O₂ on the removal of CAP (experimental conditions: initial pH = 6.8; initial CAP conc. = 110 mg/L; nZVI dosage = 1.0 g/L; 25 ± 1 °C).

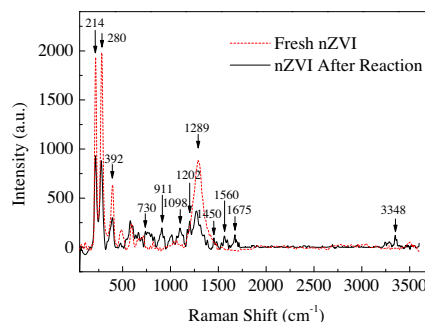


Fig. 6. Raman spectra of nZVI surfaces before and after reaction with CAP.

as an important parameter in the process of CAP removal. There was probably Fenton reaction occurring on the nZVI in the presence of air, which can produce strong oxidants, such as hydroxyl

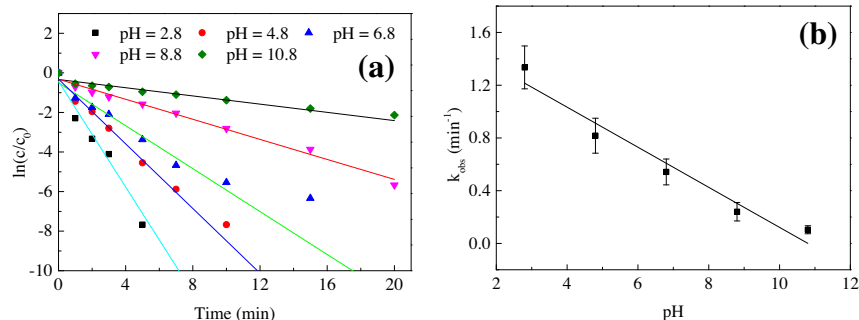


Fig. 4. (a) Effects of variations in initial pH on the removal of CAP (experimental conditions: initial CAP conc. = 110 mg/L; nZVI dosage = 1.0 g/L; shaking speed = 150 rpm; 25 ± 1 °C); (b) relationship between initial pH and observed rate coefficients.

Table 1
Possible vibration for Raman shifts.

Raman shift (cm ⁻¹)	Possible vibration
730	C–Cl
911	C–C
1098	C–C
1202	Para disubstituted benzenes
1450	–CH ₃
1560	–NO ₂
1675	Amide I
3348	–NH ₂

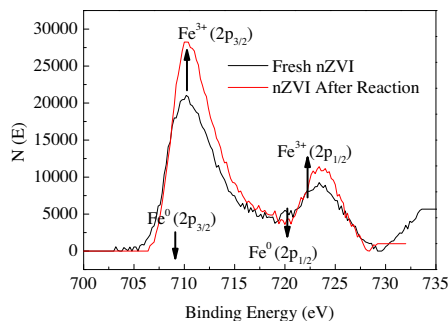


Fig. 7. XPS spectra of nZVI surfaces before and after reaction with CAP.

radicals ($\cdot\text{OH}$) [37,38]. This result demonstrates that the CAP removal by nZVI could be undertaken in a system open to the atmosphere and enhanced by the presence of oxygen.

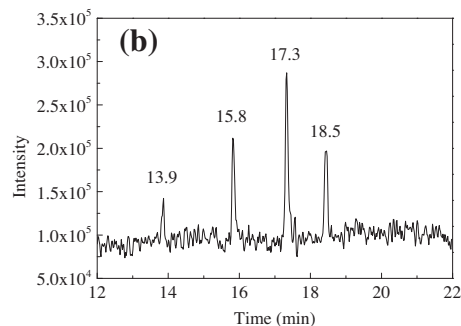
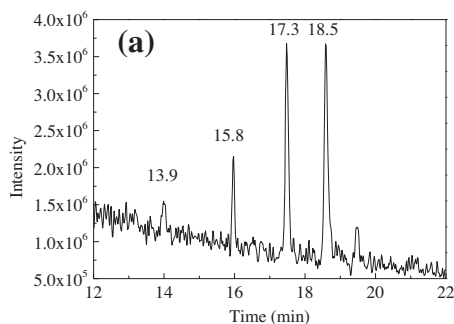


Fig. 8. LC-MS chromatograms of CAP reduction products (a) Positive Ion; (b) Negative Ion.

Table 2
Detected potential CAP reduction products via LC-MS.

Compound	Molecular weight	Formula	Potential structure
I	288	C ₁₁ H ₁₃ ClN ₂ O ₅	
II	224	C ₁₁ H ₁₆ N ₂ O ₃	

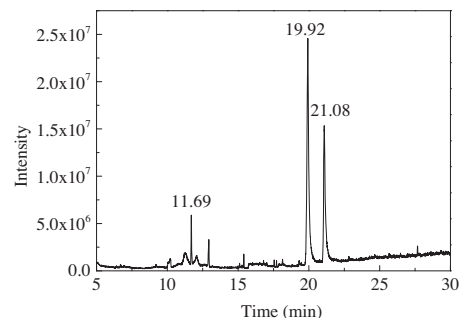


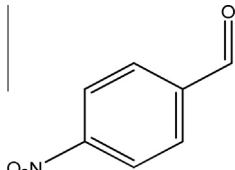
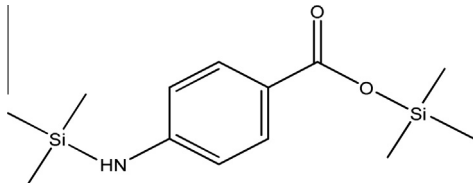
Fig. 9. GC-MS chromatogram of CAP reduction products.

3.3. Change in characterization of nZVI before and after the reaction

Fig. 6 shows Raman spectra for nZVI before and after reaction with CAP. Fresh nZVI shows bands at 217, 280, 399, 590 and 1289 cm⁻¹. After the reaction, the bands for iron oxides declined and new bands were evident at 730, 911, 1098, 1202, 1450, 1560, 1675, and 3348 cm⁻¹. As shown in Table 1, the new bands indicated the presence of the corresponding organic functional groups on the nZVI surface, which should be related to the reduction products of CAP. For example, the presence of –NH₂ should be attributed to –NO₂ reduction of CAP [39–41]. The results indicated that adsorption and deoxidization of CAP took place on the surface of nZVI.

Fig. 7 presents XPS spectra for the narrow scan of Fe (2p). For the fresh nZVI, the photoelectron peaks at 707 and 720 eV represent the 2p_{3/2} peaks and 2p_{1/2} of Fe⁰, respectively. The peaks at 710 and 724 eV represent the binding energies of Fe³⁺ (2p_{3/2}) and shake-up satellite 2p_{1/2}, respectively. The two main feature peaks

Table 3
Detected derivatization compounds of CAP reduction products via GC–MS.

Compound	Molecular weight	Formula	Potential structure
III	151	C ₇ H ₅ NO ₃	
IV	281	C ₁₃ H ₂₃ NO ₂ Si ₂	

suggested that the surface of the iron nanoparticles mainly consisted of a layer of iron oxides, probably in the form of FeO or Fe₂O₃ [42,43]. It was possible that samples were exposed to air during the test, resulting in the oxidation of some of the nZVI surfaces. For the nZVI after reaction, the photoelectron peaks at 710 and 724 eV represent the binding energies of Fe (2p_{3/2}) and shake-up satellite 2p_{1/2}, respectively, and the Fe⁰ feature peaks disappeared. As the XPS technique was used to study sample surface properties at depth of 3–5 nm, it can be assumed that the reacted nZVI was covered by an iron oxide film that was thicker than 5 nm.

ICP results showed that there was 30.7 mg/L soluble Fe in the solution after 20 min of reaction (experiment conditions: initial pH 6.8, initial CAP 110 mg/L, nZVI dosage 1.0 g/L and 25 ± 1 °C), whereas only 9.9 mg/L was in the solution of nZVI-blank after the same period. This result indicates that part of nZVI was oxidized and dissolved in the solution during the reaction.

The XPS analysis along with the ICP results demonstrate that iron oxides and hydroxides were formed both on the nZVI surface and in the solution, which denotes the occurrence of redox reaction.

3.4. Analyses of reduction products

As an electron donor, nZVI is effective in transforming of a wide array of common environmental contaminants such as chlorinated solvents, heavy metal ions and organic dyes due to its strong reductive characteristics [9]. The reduction products of CAP after treatment by nZVI were analyzed by using LC–MS. Four new peaks were observed at retention time of 13.9, 15.8, 17.3 and 18.5 min (Fig. 8). Based on LC–MS results, the possible reduction products of CAP by nZVI are proposed in Table 2. Compound I (MW 288, 15.8 min) originated from CAP reduction via loss of chlorine due to the low bond energy of C–Cl. Further reduction of Compound I lead to the generation of Compound II (MW 224, 13.9 min) via further dechlorination and nitro group reduction. To our best knowledge, other two peaks at retention time of 17.3 and 18.5 min still remain unclear, which could be multimers generated during electrospray ionization.

For further investigation of the reduction products of CAP, experiments were performed using GC–MS with the solution after extraction and derivatization. Fig. 9 presents the GC–MS spectra of the solution after reaction. Three obvious flow peaks were observed at retention times of 11.69, 19.92, and 21.08 min. Compound III (MW 151, SI 930, RSI 930, Prob. 80.38%) and Compound IV (MW 281, SI 730, RSI 824, Prob. 62.74%) in Table 3 were found in the reference of NIST/EPA/NIH Mass Spectral Library, at the retention times of 11.69 and 19.92 min, respectively. The high match possibility means both Compound III and IV have

characteristic fragments similar to the actual reduction products of CAP. Compound IV contains an amide group, which could originate from the silylation derivatives of Compound II with a shortened side chain. Thus the GS–MS results provided an indirect proof of Compound II as potential transformation products of CAP.

According to the above results, the potential reduction routine of CAP by nZVI can be proposed as following. CAP was dechlorinated by nZVI to Compound I in the first place, which was further converted to Compound II with further dechlorination and nitro group reduction.

4. Conclusions

The present study demonstrates that nZVI can be used to efficiently remove antibiotic CAP from aqueous solution. The CAP removal by nZVI followed the pseudo-first-order kinetics model. The removal efficiency was enhanced with increasing nZVI dosage and decreasing pH. The nZVI/air process showed a faster removal rate compared with the nZVI/N₂ process. The Raman spectra showed the adsorption and deoxidization of CAP on the surface of nZVI. The XPS and ICP results further confirmed the occurrence of reduction reaction. From the LC–MS and GC–MS results of the CAP reduction products, dechlorination followed by nitro group reduction was proposed to be the potential reduction routine of CAP by nZVI.

Acknowledgements

The authors sincerely thank the supports of the National Science & Technology Pillar Program (2013BAD21B03), China Scholarship Council, the Fundamental Research Funds for the Central Universities, and the higher school innovative engineering plan (111 Project).

References

- [1] M. Rabiet, A. Togola, F. Brissaud, J.-L. Seidel, H. Budzinski, F. Elbaz-Poulichet, Consequences of treated water recycling as regards pharmaceuticals and drugs in surface and ground waters of a medium-sized Mediterranean catchment, *Environ. Sci. Technol.* 40 (2006) 5282–5288.
- [2] N. Nakada, K. Kiri, H. Shinohara, A. Harada, K. Kuroda, S. Takizawa, H. Takada, Evaluation of pharmaceuticals and personal care products as water-soluble molecular markers of sewage, *Environ. Sci. Technol.* 42 (2008) 6347–6353.
- [3] P.K. Jjemba, Excretion and ecotoxicity of pharmaceutical and personal care products in the environment, *Ecotoxicol. Environ. Saf.* 63 (2006) 113–130.
- [4] F. Gagné, C. Blaise, C. André, Occurrence of pharmaceutical products in a municipal effluent and toxicity to rainbow trout (*Oncorhynchus mykiss*) hepatocytes, *Ecotoxicol. Environ. Saf.* 64 (2006) 329–336.
- [5] R. Reza, M. Ahmaruzzaman, A.K. Sil, V.K. Gupta, Comparative adsorption behaviour of Ibuprofen and Clofibrac acid onto microwave assisted activated bamboo waste, *Ind. Eng. Chem. Res.* (2014).

- [6] R. Reza, J.K. Ahmed, A.K. Sil, M. Ahmaruzzaman, A non-conventional adsorbent for the removal of Clofibrac acid from aqueous phase, *Sep. Sci. Technol.* (2014).
- [7] P. Liu, H. Zhang, Y. Feng, F. Yang, J. Zhang, Removal of trace antibiotics from wastewater: a systematic study of nanofiltration combined with ozone-based advanced oxidation processes, *Chem. Eng. J.* 240 (2014) 211–220.
- [8] B. Kasprzyk-Hordern, R.M. Dinsdale, A.J. Guwy, The removal of pharmaceuticals, personal care products, endocrine disruptors and illicit drugs during wastewater treatment and its impact on the quality of receiving waters, *Water Res.* 43 (2009) 363–380.
- [9] P.S. Lovett, Translation attenuation regulation of chloramphenicol resistance in bacteria – a review, *Gene* 179 (1996) 157–162.
- [10] B.E. Wiholm, J.P. Kelly, D. Kaufman, S. Issaragrisil, M. Levy, T. Anderson, S. Shapiro, Relation of aplastic anaemia to use of chloramphenicol eye drops in two international case-control studies, *Br. Med. J.* 316 (1998). 666–666.
- [11] H. Liu, G. Zhang, C.-Q. Liu, L. Li, M. Xiang, The occurrence of chloramphenicol and tetracyclines in municipal sewage and the Nanming River, Guiyang City, China, *J. Environ. Monit.* 11 (2009) 1199–1205.
- [12] R. Hirsch, T. Ternes, K. Haberer, K.-L. Kratz, Occurrence of antibiotics in the aquatic environment, *Sci. Total Environ.* 225 (1999) 109–118.
- [13] A. Chatzidakis, C. Berberidou, I. Paspaltsis, G. Kyriakou, T. Sklaviadis, I. Poullos, Photocatalytic degradation and drug activity reduction of chloramphenicol, *Water Res.* 42 (2008) 386–394.
- [14] J.W. Zhang, D.F. Fu, Y.D. Xu, C.Y. Liu, Optimization of parameters on photocatalytic degradation of chloramphenicol using TiO₂ as photocatalyst by response surface methodology, *J. Environ. Sci. China* 22 (2010) 1281–1289.
- [15] S. Kapoor, L. Varshney, Redox reactions of chloramphenicol and some aryl peroxy radicals in aqueous solutions: a pulse radiolytic study, *J. Phys. Chem. A* 101 (1997) 7778–7782.
- [16] T. Csay, G. Racz, E. Takacs, L. Wojnarovits, Radiation induced degradation of pharmaceutical residues in water: chloramphenicol, *Radiat. Phys. Chem.* 81 (2012) 1489–1494.
- [17] F. Xie, Research on irradiation-induced degradation products and mechanism of chloramphenicol in animal derived food, in: *Institute of Agro-Products Processing Science and Technology, Chinese Academy of Agricultural Science, Beijing, 2008*, pp. 16–34.
- [18] Z.Q. Fang, J.H. Chen, X.H. Qiu, X.Q. Qiu, W. Cheng, L.C. Zhu, Effective removal of antibiotic metronidazole from water by nanoscale zero-valent iron particles, *Desalination* 268 (2011) 60–67.
- [19] Y. Fan, B. Wang, S.H. Yuan, X.H. Wu, J. Chen, L.L. Wang, Adsorptive removal of chloramphenicol from wastewater by NaOH modified bamboo charcoal, *Bioresour. Technol.* 101 (2010) 7661–7664.
- [20] R. Crane, T. Scott, Nanoscale zero-valent iron: future prospects for an emerging water treatment technology, *J. Hazard. Mater.* 211 (2012) 112–125.
- [21] J. Farrell, N. Melitas, M. Kason, T. Li, Electrochemical and column investigation of iron-mediated reductive dechlorination of trichloroethylene and perchloroethylene, *Environ. Sci. Technol.* 34 (2000) 2549–2556.
- [22] S.H. Joo, A.J. Feitz, T.D. Waite, Oxidative degradation of the carbothioate herbicide, molinate, using nanoscale zero-valent iron, *Environ. Sci. Technol.* 38 (2004) 2242–2247.
- [23] C.R. Keenan, D.L. Sedlak, Factors affecting the yield of oxidants from the reaction of nanoparticulate zero-valent iron and oxygen, *Environ. Sci. Technol.* 42 (2008) 1262–1267.
- [24] C. Lee, D.L. Sedlak, Enhanced formation of oxidants from bimetallic nickel–iron nanoparticles in the presence of oxygen, *Environ. Sci. Technol.* 42 (2008) 8528–8533.
- [25] C. Noubactep, A critical review on the process of contaminant removal in Fe-0-H₂O systems, *Environ. Technol.* 29 (2008) 909–920.
- [26] C.B. Wang, W.X. Zhang, Synthesizing nanoscale iron particles for rapid and complete dechlorination of TCE and PCBs, *Environ. Sci. Technol.* 31 (1997) 2154–2156.
- [27] G.N. Glavee, K.J. Klabunde, C.M. Sorensen, G.C. Hadjipanayis, Chemistry of borohydride reduction of iron(II) and iron(III) ions in aqueous and nonaqueous media – formation of nanoscale Fe, Fe₂, and Fe₂O₃ powders, *Inorg. Chem.* 34 (1995) 28–35.
- [28] K.P. Singh, A.K. Singh, S. Gupta, P. Rai, Modeling and optimization of reductive degradation of chloramphenicol in aqueous solution by zero-valent bimetallic nanoparticles, *Environ. Sci. Pollut. R* 19 (2012) 2063–2078.
- [29] H. Chen, H.J. Luo, Y.C. Lan, T.T. Dong, B.J. Hu, Y.P. Wang, Removal of tetracycline from aqueous solutions using polyvinylpyrrolidone (PVP-K30) modified nanoscale zero valent iron, *J. Hazard. Mater.* 192 (2011) 44–53.
- [30] M. Stieber, A. Putschew, M. Jekel, Treatment of pharmaceuticals and diagnostic agents using zero-valent iron – kinetic studies and assessment of transformation products assay, *Environ. Sci. Technol.* 45 (2011) 4944–4950.
- [31] B.L. Cushing, V.L. Kolesnichenko, C.J. O'Connor, Recent advances in the liquid-phase syntheses of inorganic nanoparticles, *Chem. Rev.* 104 (2004) 3893–3946.
- [32] S. Bae, W. Lee, Inhibition of nZVI reactivity by magnetite during the reductive degradation of 1,1,1-TCA in nZVI/magnetite suspension, *Appl. Catal. B Environ.* 96 (2010) 10–17.
- [33] S.M. Ponder, J.G. Darab, T.E. Mallouk, Remediation of Cr(VI) and Pb(II) aqueous solutions using supported, nanoscale zero-valent iron, *Environ. Sci. Technol.* 34 (2000) 2564–2569.
- [34] X. Zhang, Y.M. Lin, Z.L. Chen, 2,4,6-Trinitrotoluene reduction kinetics in aqueous solution using nanoscale zero-valent iron, *J. Hazard. Mater.* 165 (2009) 923–927.
- [35] W.H. Zhang, X. Quan, J.X. Wang, Z.Y. Zhang, S. Chen, Rapid and complete dechlorination of PCP in aqueous solution using Ni–Fe nanoparticles under assistance of ultrasound, *Chemosphere* 65 (2006) 58–64.
- [36] G.N. Jovanovic, P. Znidarsic-Plazl, P. Sakrithichai, K. Al-Khaldi, Dechlorination of p-chlorophenol in a microreactor with bimetallic Pd/Fe catalyst, *Ind. Eng. Chem. Res.* 44 (2005) 5099–5106.
- [37] S.-H. Chang, K.-S. Wang, S.-J. Chao, T.-H. Peng, L.-C. Huang, Degradation of azo and anthraquinone dyes by a low-cost Fe-0/air process, *J. Hazard. Mater.* 166 (2009) 1127–1133.
- [38] C.E. Noradoun, I.F. Cheng, EDTA degradation induced by oxygen activation in a zerovalent iron/air/water system, *Environ. Sci. Technol.* 39 (2005) 7158–7163.
- [39] D. Colón, E.J. Weber, J.L. Anderson, P. Winget, L.A. Suárez, Reduction of nitrosobenzenes and N-hydroxylanilines by Fe (II) species: elucidation of the reaction mechanism, *Environ. Sci. Technol.* 40 (2006) 4449–4454.
- [40] P. Larese-Casanova, M.M. Scherer, Abiotic transformation of hexahydro-1,3,5-trinitro-1,3,5-triazine (RDX) by green rusts, *Environ. Sci. Technol.* 42 (2008) 3975–3981.
- [41] Z.Q. Fang, X.Q. Qiu, J.H. Chen, X.H. Qiu, Degradation of metronidazole by nanoscale zero-valent metal prepared from steel pickling waste liquor, *Appl. Catal. B Environ.* 100 (2010) 221–228.
- [42] Y.P. Sun, X.Q. Li, J.S. Cao, W.X. Zhang, H.P. Wang, Characterization of zero-valent iron nanoparticles, *Adv. Colloid Interface* 120 (2006) 47–56.
- [43] J.A. Mielczarski, G.M. Atenas, E. Mielczarski, Role of iron surface oxidation layers in decomposition of azo-dye water pollutants in weak acidic solutions, *Appl. Catal. B Environ.* 56 (2005) 289–303.